molecular
systems
biology

REVIEW

Theoretical and experimental approaches to understand morphogen gradients

Marta Ibañes[1] and Juan Carlos Izpisúa Belmonte[2,3,*]

[1] Department of Estructura i Constituents de la Matèria, University of Barcelona, Barcelona, Spain,
[2] Gene Expression Laboratory, Salk Institute for Biological Studies, La Jolla, CA, USA and
[3] Centre of Regenerative Medicine in Barcelona, Barcelona, Spain
* Corresponding author. Gene Expression Laboratory, Salk Institute for Biological Studies, 10010 North Torrey Pines Road, La Jolla, CA 92037, USA. Tel.: +1 858 453 4100 Ext. 1130; Fax: +1 858 453 2573; E-mails: belmonte@salk.edu or izpisua@cmrb.eu

Morphogen gradients, which specify different fates for cells in a direct concentration-dependent manner, are a highly influential framework in which pattern formation processes in developmental biology can be characterized. A common analysis approach is combining experimental and theoretical strategies, thereby fostering relevant data on the dynamics and transduction of gradients. The mechanisms of morphogen transport and conversion from graded information to binary responses are some of the topics on which these combined strategies have shed light. Herein, we review these data, emphasizing, on the one hand, how theoretical approaches have been helpful and, on the other hand, how these have been combined with experimental strategies. In addition, we discuss those cases in which gradient formation and gradient interpretation at the molecular and/or cellular level may influence each other within a mutual feedback loop. To understand this interplay and the features it yields, it becomes essential to take system-level approaches that combine experimental and theoretical strategies.
Molecular Systems Biology 25 March 2008; doi:10.1038/msb.2008.14
Subject Categories: development
Keywords: gradient; interpretation; modelling; morphogen; transport

Introduction

Embryonic development involves spatial and temporal patterns of cellular differentiation and the shaping of form.

How do embryonic tissues organize in space and time such that a field of distinct cells emerges reliably? This question has fascinated developmental biologists for decades. Early in the last century, the existence of gradients that could signal over large distances was proposed to account for patterning (Morgan, 1901). Indeed, morphogen gradients, defined as graded distributions of secreted molecules that specify distinct fates for the cells in a concentration-dependent and direct manner (Wolpert, 1969), have become, over the last few decades, a highly influential framework to test and understand pattern formation processes during embryonic development (Figure 1A).

The concept that the fate of cells depends on their spatial position, enabling an organized pattern to arise, was formalized by Lewis Wolpert in his positional information model (Wolpert, 1969). According to this model, cells have their spatial position specified along specific directions with respect to one or more reference points and translate such positional information into specific cell behaviours, which depend, as well, on the developmental history of the cell. Which kind of signals could provide positional information to the cells? Wolpert envisaged spatial gradients of a chemical's concentration over a field of cells as one of the potential signals: cells that sense a low amount of chemical are more distant from the reference point (i.e. the source of the chemical) than cells that sense a higher amount.

The first molecular demonstration of the concept of gradients specifying distinct fates in a direct manner took time to appear and was provided in the *Drosophila* syncytium (Driever and Nüsslein-Volhard, 1988a, b). The transcription factor Bicoid was shown to be distributed along a gradient expanding from the anterior pole to more than one-half of the embryo and to regulate the expression of downstream gap genes (for a review, see Ephrussi and Johnston, 2004). Afterwards, other signalling proteins such as Dpp, Wingless, Spitz, Hedgehog, Activin and Nodal have been described as morphogens in a wide variety of organisms (for reviews, see Green, 2002; Martinez Arias, 2003; Tabata and Takei, 2004; Schier and Talbot, 2005; Affolter and Basler, 2007). It is worth stressing, however, that the case of Bicoid is a rather unusual one. Whereas the above-mentioned morphogens correspond to secreted molecules that can form gradients extracellularly, Bicoid is a transcription factor that forms a gradient before cellularization in the *Drosophila* embryo, from a localized region of transcription in the anterior pole.

To check whether a gradient acts as a morphogen, it is important to unveil whether it specifies distinct fates over space in a direct manner. Accordingly, experimental designs that evaluate the direct action and, hence, the requirement of the morphogen molecule at long distances have been elaborated (for a review, see Tabata and Takei, 2004). In addition, the shape of gradients has been altered by
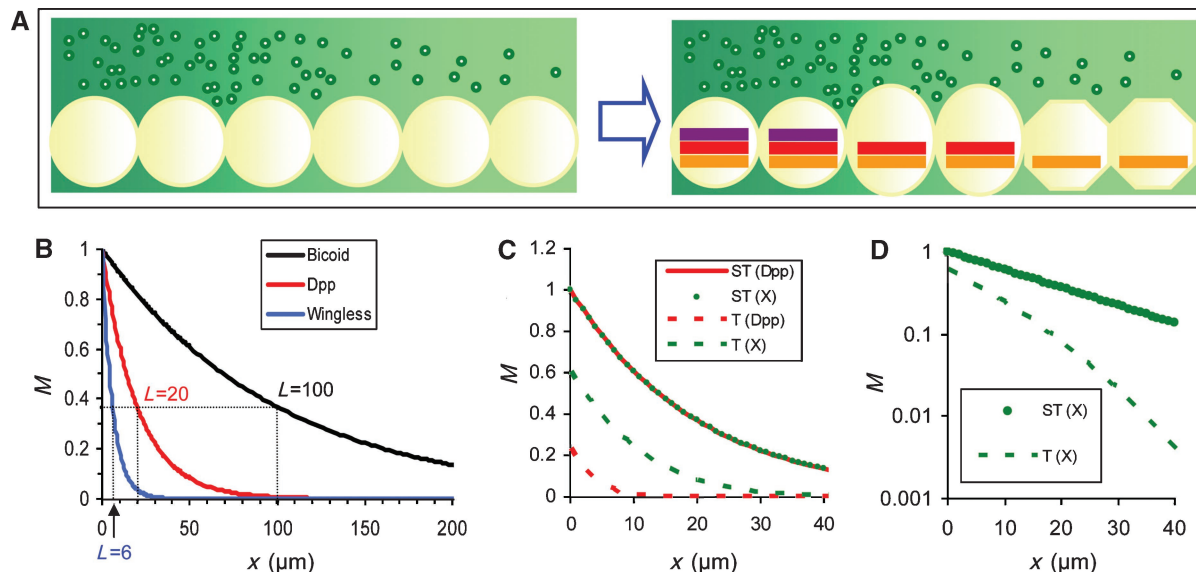
Figure 1 Dynamics and steady state of morphogen gradients. (**A**) Morphogen gradients specify a pattern in a field of cells. (Left) All cells (yellow big circles) are equivalent and a morphogen gradient is set (small green circles). Over time (blue arrow), cells respond directly to the graded concentration of a secreted molecule and a pattern (right) is specified. (Right) Depending on the amount of graded signal, distinct genes become expressed within cells (represented by different colours inside cells) and different cellular behaviours are elicited (represented by different shapes of cells). (**B**) Bicoid, Dpp and Wingless gradients are represented by exponential profiles with their corresponding characteristic length (L). M stands for the morphogen level and x for the spatial position. (**C**) Transient (T) and steady-state (ST) gradients for two different molecules (simulating Dpp in red and a molecule X in green) that have different diffusion and degradation rates but the same characteristic length in the steady-state profile ($L=20\ \mu m$). Transient gradients are computed at the same time point but, as shown, are distinct. Red curves were obtained by using the diffusion and degradation rates of Dpp. Green curves were computed by setting the molecular half-life eight times shorter than that of Dpp and the diffusion rate eight times larger. (**D**) Shape of the gradient profile at a transient time (T) and at the steady state (ST) in logarithmic spatial scale for parameter values of Dpp. The features of the gradients at the two time points are very distinct. In panels B and C, the morphogen level has been scaled such that the steady state has a morphogen level of 1 at the source ($x=0$). Profiles in panels C and D have been computed numerically according to $\partial M(x,t)/\partial t=\alpha\partial(x)+D\partial^2 M/\partial x^2-\beta M$ with an impermeable wall at $x=0$.

changing the level of the morphogen signal (Shimizu and Gurdon, 1999; Ashe *et al*, 2000) to observe whether spatial shifts in the fates of cells and in the expression pattern of target genes arise (Ashe and Briscoe, 2006). Hence, as it is expected from a morphogen, changes in Bicoid concentration along its gradient elicit shifts in the expression domain of its downstream target gap genes and alter the fate of cells (Driever and Nüsslein-Volhard, 1988a; Driever *et al*, 1989a, c; Driever and Nüsslein-Volhard, 1989b; Struhl *et al*, 1989; St Johnston and Nüsslein-Volhard, 1992; Rivera-Pomar and Jäckle, 1996).

Although other frameworks for patterning processes have been proposed (Turing, 1952), morphogen gradients have been the most influential up to now, stimulating and promoting strategies to unveil the process of embryonic patterning. Hence, graded signals have been searched and evaluated for a morphogen-like role in many patterning developmental processes. Although most studies on the visualization, quantification and interpretation of gradients have been developed in *Drosophila* embryos, the relevance of morphogens in vertebrate embryonic development has also been taken into account, as exemplified by models for limb patterning (Izpisúa-Belmonte *et al*, 1991; Tickle, 1999; Tabin and Wolpert, 2007). Indeed, morphogen gradients on vertebrate systems have become a focus of increasing interest (Chen and Schier, 2001; Dubrulle and Pourquié, 2004; Dessaud *et al*, 2007; Simeoni and Gurdon, 2007; White *et al*, 2007).

At present, the development of novel experimental and visualizing techniques has enabled refined measurements of the spatially graded distribution of molecules along tissues.

Accordingly, combined experimental and computational strategies that quantify and characterize the formation of gradients as well as theoretical approaches that address open issues related to the properties of gradients have become a common approach (see, for instance, Kerszberg and Wolpert, 1998; Eldar *et al*, 2002, 2003, 2006; Lander *et al*, 2002, 2007; Jaeger *et al*, 2004; Kruse *et al*, 2004; Aegerter-Wilmsen *et al*, 2005; Bollenbach *et al*, 2005; England and Cardy, 2005; Houchmandzadeh *et al*, 2005; Howard and ten Wolde, 2005; Melen *et al*, 2005; Mizutani *et al*, 2005; Shimmi *et al*, 2005; Ibañes *et al*, 2006; McHale *et al*, 2006; Umulis *et al*, 2006; Bergmann *et al*, 2007; Gregor *et al*, 2007a, b; Kicheva *et al*, 2007). However, as we have learned more about morphogen gradients and their role in shaping the embryo, new complexities have emerged. Herein, we examine these issues, highlighting those recent findings that unveil novel aspects of morphogen gradients with an emphasis on how theoretical and computational studies have contributed. Moreover, we discuss how these findings emphasize the need for taking new approaches that utilize experimental and theoretical strategies to integrate both the formation and interpretation of morphogen gradients into a single framework.

A wide variety of molecular gradients

During the last few decades, gradients of different kinds of molecules, with a wide variety of sizes and dynamics, have been uncovered, revealing that both the morphogen and the

underlying tissue over which the gradient expands determine its features as well (Gurdon *et al*, 1994; Nellen *et al*, 1996; Entchev *et al*, 2000; Strigini and Cohen, 2000; Teleman and Cohen, 2000; Dorfman and Shilo, 2001; McDowell *et al*, 2001; Houchmandzadeh *et al*, 2002; Gregor *et al*, 2005, 2007b; Bollenbach *et al*, 2007).

The visualization of the protein gradient is the first step in detecting a morphogen. To this end, antibody staining and GFP fusion proteins, among others, have been used to provide a static image of the gradient on fixed tissue. Attaining more detailed measurements has allowed quantification of morphogen gradients. Specifically, imaging of functional fluorescent green protein-morphogen fusions over space has shown that Bicoid in the *Drosophila* syncytium and Dpp and Wingless in the fly's wing form gradients with the same kind of decay characterized by an exponential shape. This kind of profile implies that the fraction of morphogen that decreases over space is the same all over the gradient. Accordingly, a single scale characterizes the spatial decay and it can be used as a measure of its size. By fitting an exponential profile to the fluorescent data, a characteristic length of the gradient can be obtained. This procedure has shown that the Bicoid gradient is much larger, with a characteristic length of 100 μm, than the Dpp and Wingless gradients, which have a characteristic length of 20 and 6 μm, respectively (Houchmandzadeh *et al*, 2002; Kicheva *et al*, 2007) (Figure 1B). Activity gradients have been monitored as well by measuring the amounts of downstream intracellular responses (e.g. kinase phosphorylation). This is the case of the BMP gradient, which patterns the dorsoventral axis in *Drosophila* embryos. This gradient shows a sharp profile that decays strongly over a field of five cells and is formed within 30 min (Eldar *et al*, 2002; Mizutani *et al*, 2005).

Once the gradient profile has been fitted, it remains to be elucidated which dynamic yields it. Mathematical and numerical modelling can be very helpful to this end (Box 1; Figure 2A and B). In addition, theoretical approaches can also enable the quantification of the dynamics taking place. For instance, an exponential gradient profile is the steady-state solution of a morphogen dynamic involving diffusion and linear degradation. Taking into account that diffusion rates have dimensions of surface over time and degradation rates of the inverse of time, a dimensional analysis of this dynamic readily reveals that the characteristic length of the gradient depends on these parameters as $\sqrt{D/\beta}$, where D and β are the diffusion and degradation rates, respectively. Therefore, all those different values of D and β rates that yield the same ratio D/β elicit a steady-state gradient spanning the same spatial region (Figure 1C). Conversely, by quantifying the characteristic length of the gradient through the data on the gradient profile, we cannot infer which values of the diffusion and degradation rates underlie the morphogen dynamics. However, the transient dynamics may depend on the diffusion rate D on its own (Figure 1C and D). Thus, we can obtain the value of D by measuring this dynamic. This is the approach used by Kicheva *et al* (2007) to characterize the kinetics of the Dpp and Wingless gradients. The authors measured the fluorescence recovery after photobleaching (FRAP) during a time interval of 1 h. FRAP experiments were modelled, taking into account both production and degradation processes, and the

Box 1 Gradient formation inference: some examples

Mathematical and numerical analyses enable us to make hypotheses on the mechanisms underlying the formation of a gradient and to predict the profile of the gradient that arises accordingly. However, different mechanisms can yield the same or rather similar profiles, when measured experimentally. For instance, Bicoid, Dpp and Wingless all show approximately an exponential profile. However, the mechanisms controlling their formation differ strongly. Whereas Bicoid transport occurs in the cytoplasm and through nuclear membranes, transcytosis can play a key role in Dpp transport (Kicheva *et al*, 2007; Gregor *et al*, 2007b). Therefore, it becomes difficult to discern which mechanism is acting by just looking at the shape of the gradient. But we can manipulate the gradient to obtain more information on how it is formed. We can model mathematically and numerically this manipulation and predict the dynamics that are expected to occur when a specific mechanism of gradient formation is assumed. Then, we can compare this prediction with the actual measurements.

For instance, gradient dynamics involving transport driven by diffusion or by progeny cells moving away from their proliferating source can both yield an exponential profile. However, the mathematical derivation of these profiles reveals that their characteristic lengths depend distinctly on the lifetime of the molecule (Ibañes *et al*, 2006). Indeed, the characteristic length of the diffusion-driven gradient increases much less when the lifetime becomes longer than for the cell-based transport gradient. Thus, we could potentially test the mechanism of transport by altering the lifetime of the molecule and measuring the change in the characteristic length of the gradient. Another example is given by gradients formed through diffusion but by distinct mechanisms of degradation. When the degradation rate is uniform over space, an exponential gradient profile at the steady state arises. However, when degradation is differentially modulated over space (e.g. by the morphogen signalling, which promotes its own degradation), a profile with strong decay close to the source and long tails is formed (Eldar *et al*, 2003). Even if these profiles were difficult to be distinguished experimentally, we could potentially test the mechanism of degradation by altering the rate of production at the source (Figure 2A). When the mathematical expressions of the profiles are written down, we find out that the amount of morphogen at the source is proportional to the production rate only if degradation is uniform (Figure 2B). Thus, by altering *in vivo* the rate of production, measuring the amount of morphogen at or close to the source and checking their dependence, we can potentially gain insights into how the degradation proceeds. However, and even if the experimental manipulations can be addressed, it might be not as simple as it seems, as exemplified by the studies on the Dpp gradient in the *Drosophila* wing (see main text).

Another approach is to infer the parameters characterizing each of the factors acting on the formation of a gradient (the rates of source production, transport and degradation) by measuring its dynamics and profile. Once these parameter values have been found, we can introduce modifications in those processes that we want to test and infer again new parameter values. For instance, the kinetic parameter values for the Dpp gradient in the fly's wing have been inferred assuming a random diffusion-like transport (Kicheva *et al*, 2007; see main text for a description of the procedure). The authors also wanted to test if transcytosis was eliciting any transport. Accordingly, they impaired the endocytic pathway and under this condition performed the same kind of measurements they used to infer the kinetic parameter values. The values obtained when endocytosis was impaired revealed that both the degradation and transport rates of Dpp became reduced, therefore supporting a role of transcytosis in driving Dpp transport (Kicheva *et al*, 2007).

mathematical expression of the recovery dynamics, with their dependence on the kinetic morphogen parameters, was formulated. Importantly, the recovery dynamics depend on the diffusion rate D and not just on the characteristic length (Kicheva *et al*, 2007). By adjusting the mathematically derived expressions of the recovery dynamics with the measured FRAP data over time and space, Kicheva *et al* found the value of D. Moreover, as the characteristic length was also known from the gradient profile data, the degradation rate β could be inferred (Kicheva *et al*, 2007). Note that for the sake of
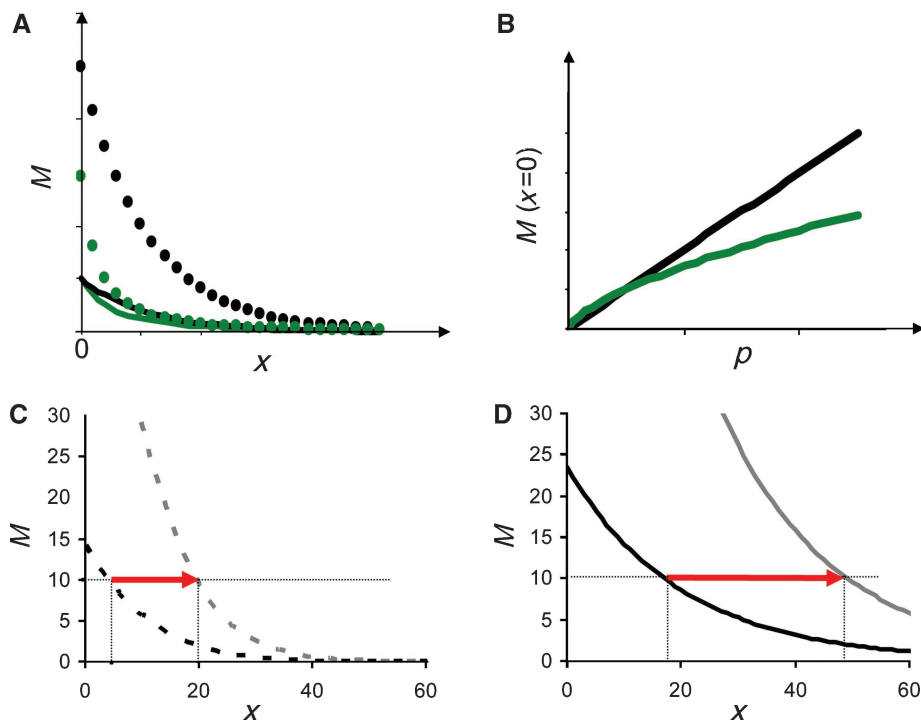
Figure 2 Gradient responses to perturbations. Responses of gradients to changes in the production rate *p* at the source. (**A**) Steady-state gradient profiles for two types of gradients (green, black) and for two different production rates (lines for *p*=1 and circles for *p*=5). Gradients formed by diffusion and linear degradation are depicted in black (exponential profile), whereas those formed by diffusion and nonlinear (enhanced) degradation are depicted in green (power-law profile). Two quite similar steady-state gradient profiles (green and black lines) become much more distinct when the production rate is increased by a factor of 5 (green and black circles). (**B**) Steady-state morphogen level at the source as a function of the production rate *p* for the two types of gradients analysed in panel A. The qualitative dependence is shown. Power 2 is used for nonlinear degradation. (**C, D**) Gradient profiles formed by diffusion and linear degradation for *p*=1 (black) and *p*=5 (grey) at a transient dynamical stage (C) and at the steady state (D). The dotted horizontal lines denote a threshold of morphogen level. Red arrows denote the spatial shift that is elicited when the production rate increases. Vertical dotted lines denote the spatial position where the threshold is located. The shift is much larger at the steady state than at a transient state. Also note that the spatial position is different at the transient state and at the steady state. See Bergmann *et al* (2007) for a study of these features on the Bicoid gradient. Panels C and D use the same parameter values except for *p*. Profiles in panels A and B are computed from analytical expressions from Eldar *et al* (2003). Panels C and D are computed as in Figure 1.

simplicity and clarity, herein we have sketched the approach that in the original work was much more complex and involved several parameters to be determined.

Assigning quantitative values to the kinetics of the Dpp and Wingless gradients allows pinpointing which element is responsible for the shorter spatial range of the Wingless gradient: does Wingless diffuse much less than Dpp or does it have a much shorter half-life? The study by Kicheva *et al* (2007) showed that the short half-life of Wingless (8 min) compared with the 45 min half-life of Dpp yields a Wingless gradient spanning much fewer cells, whereas the effective diffusion rates are rather similar between both morphogens ($D \approx 0.1\,\mu m^2/s$ for Dpp and ($D \approx 0.5\,\mu m^2/s$ for Wingless).

The numerical solution for the dynamics of morphogen diffusion from a localized source of production and linear morphogen degradation shows that the morphogen gradient achieves a steady state over a broad spatial region on time periods one order of magnitude longer than the morphogen half-life (Bergmann *et al*, 2007). Thus, by using the above-mentioned molecular half-lives, it can be reasoned that the Dpp gradient takes around 450 min to be formed, whereas Wingless forms its gradient much more rapidly, in only 80 min. This is in agreement with the time of morphogen signal
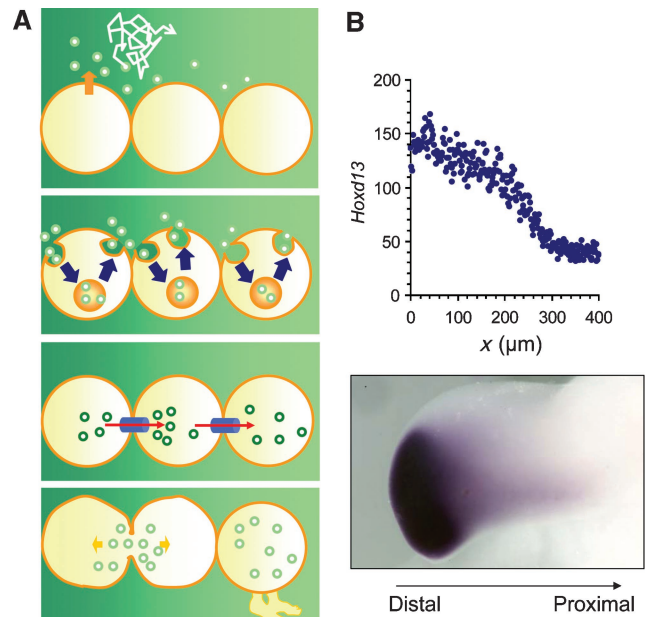
recovery after reversible blockage of the morphogen through temperature changes, which has also been used to infer how long a gradient takes to be formed (Entchev *et al*, 2000; Teleman and Cohen, 2000). Recently, *in vivo* optical imaging that allows the measurement of the whole gradient all along its formation has been implemented for the Bicoid gradient (Gregor *et al*, 1992, 2007b). The data showed that a gradient with stable nuclear concentration is formed within 90 min (Gregor *et al*, 2007b). Therefore, if the overall gradient is at a steady state and is formed by diffusion and linear degradation, we would expect the Bicoid half-life to be around 9 min and, based on the characteristic length (100 μm) of the gradient, the diffusion rate to be around $13\,\mu m^2/s$. Indeed, dextran molecules with the molecular mass of Bicoid protein diffuse in *Drosophila* embryos with a similar rate (Gregor *et al*, 2005). However, this value does not agree with the Bicoid diffusion rate inferred from fluorescent recovery dynamics at the cortex of *Drosophila* embryos, raising the open issue on how to conciliate these results (Box 2).

Recently, the formation of gradients over a field of cells has been expanded to include non-secreted molecules (Gaunt *et al*, 2003; Dubrulle and Pourquié, 2004; Ibañes *et al*, 2006). Specifically, mRNAs, such as the fibroblast growth factor *fgf8* along the anteroposterior axis of mouse and chick embryos

Box 2 Diffusion and the Bicoid gradient

To demonstrate the actual participation of diffusion as a transport mechanism for morphogen gradients, several strategies have recently been used to evaluate the Bicoid diffusion rate. The data, however, have yielded strikingly different values (Gregor *et al*, 2005, 2007b). On the one hand, inert fluorescent dextran molecules were injected in the anterior pole of the *Drosophila* syncytium and the fluorescent intensity over 1 h at different spatial positions a few hundred microns from the injection point was measured (Gregor *et al*, 2005). All these time-evolution data curves were fitted by computationally derived time courses obtained from a 3D description of diffusive transport over a domain with geometry determined by two-photon images of embryos. Analysis of the fluorescent curves was made such that the single free parameter to be fitted was the diffusion rate. Dextran molecules of several molecular masses were used, in the range of the Bicoid molecular mass, uncovering that data adjusted to a modified Stokes–Einstein relationship (i.e. diffusion rate decreases as an inverse function of molecular radius) in which diffusion is uniformly increased (Gregor *et al*, 2005). The inferred diffusion rates were in the order of 10 μm^2/s, which were in the range expected if the Bicoid gradient, with characteristic length of 100 μm, is assumed to reach the steady state within 1 h (see main text). However, direct measures of Bicoid motion have yielded a very different, much smaller, diffusion rate. By measuring Bicoid dynamic recovery 1 min after photobleaching at the cortical cytoplasm, and by fitting time-course curves obtained from a 3D diffusion-transport to these data, the Bicoid diffusion rate was inferred to be around 0.3 μm^2/s, three orders of magnitude smaller than the diffusion rate of dextran molecules (Gregor *et al*, 2007b). Note that, due to technical issues, this measure could only be made for Bicoid motion within the cortical region and at times beyond 1 h after fertilization. Can this small diffusion coefficient account for the Bicoid gradient profile? If this is the rate of Bicoid diffusion all over the time period of gradient formation (around 2 h) and all through the cytoplasm (within the bulk as well), it would imply that the Bicoid gradient does not reach a steady state, as it has been proposed (Bergmann *et al*, 2007, 2008). However, criticisms have been raised against this proposal, which argue that the diffusion coefficient driving the long-time and large-scale dynamics must be higher, as the inferred diffusion rate is too small to account for the hundreds of microns Bicoid spans in just 2 h (Gregor *et al*, 2007b; Bialek *et al*, 2008). Different diffusion rates over space (at the bulk cytoplasm and the cortex) and time (during the first hour after fertilization and thereafter), or active transport mechanisms that may yield to faster diffusion at long times have been alternatively proposed to resolve this paradox (Gregor *et al*, 2007b; Bialek *et al*, 2008). Some of the experiments and analyses that could shed light on this puzzling issue, and which are challenging due to technical limitations and difficulties they involve, are measurements of the Bicoid dynamics at the bulk of the cytoplasm and during the first hour after fertilization, measurements of the overall level of Bicoid along time at a specific spatial position, the measurement of Bicoid lifetime or of changes in the gradient when this lifetime is altered, as well as theoretical analyses that can point out the range of plausible Bicoid diffusion rates when the gradient is transient, at the steady state or driven by additional transport mechanisms.

Figure 3 Transport mechanisms for molecular gradient formation. (**A**) Cells are depicted by orange circles. Small green circles stand for the molecules forming the gradient. The transport mechanisms are described from top to bottom. (1) Molecules are secreted (orange arrow) and perform a random motion (white line) on the extracellular space; inside cells, molecules can also move randomly (not shown). (2) Endocytosis and exocytosis of vesicles (orange circles) carrying the molecule is shown; once molecules are secreted, they can diffuse (as in the top panel). Vesicles can also be secreted to the extracellular space and move, carrying the molecule (not shown). (3) Gap junctions (blue cylinder) allow the transport of specific molecules through cells (red arrow). (4) Cell division and growth (orange arrows) dilute and transport the molecule over space. The displacement and motion of cells (characterized by feet) can transport the molecule. Several of these transport mechanisms can be participating in the formation of a single molecular gradient. (**B**) Distal-to-proximal gradient of *Hoxd13* mRNA in the chick limb bud formed by cell proliferation. (Top) Average fluorescent signal along the proximodistal axis at the anterior positions. (Bottom) Whole-mount *in situ* hybridization of exonic expression domains in the forelimb at Hamburger and Hamilton stage 26. Modified from Ibañes *et al* (2006).

and the homeobox gene *Hoxd13* in the chick limb, have been shown to form gradients over large fields of cells (Dubrulle and Pourquié, 2004; Ibañes *et al*, 2006). In the case of *Hoxd13*, the gradient spans more than 400 μm and takes several hours to be formed (Figure 3B). These graded distributions of mRNA necessarily elicit protein gradients (Ibañes *et al*, 2006). These protein gradients could potentially specify (in the case of secreted proteins) or control (in the case of transcription factors) distinct cell fates. Therefore, these novel observations raise the intriguing question of whether these gradients are acting in a morphogen-like manner (i.e. by instructing directly distinct cell fates). If future investigations support such a role, then the concept of morphogen could be extended to include non-secreted proteins.

Creating a molecular gradient

Three main elements participate in the creation of a steady-state chemical gradient: the source of morphogen production, the sink and the transport of the morphogen through space. Regarding the source, focus has been mainly on local homogeneous sources of production, defined by a spatial domain where production is uniform over space and constant over time. However, non-uniform sources of protein production can also exist, arising from mRNA gradients, for instance, and which readily create protein gradients (Dubrulle and Pourquié, 2004; Ibañes *et al*, 2006).

Degradation of the molecule (or in general terms, the subtraction of the morphogen) facilitates the formation of gradients. Such degradation can be an active process in which specific proteins destroy the morphogen, or a passive dilution driven by cell division for rather stable proteins (Ibañes *et al*, 2006). The interaction of the morphogen with other molecules, for example, ligand morphogen binding and unbinding with receptors, can be re-interpreted in terms of degradation and source-like terms and, as expected, can also shape the

gradient. Recent studies have shown that morphogen degradation can be controlled by the morphogen signal, setting a feedback between gradient formation and signalling, and eliciting differential degradation over space. Invertebrate and vertebrate Hedgehog morphogen as well as retinoic acid in zebrafish embryos has been shown to make use of these feedbacks when creating morphogen gradients (Eldar *et al*, 2003; Dessaud *et al*, 2007; White *et al*, 2007). Hedgehog signalling induces the expression of its receptor, Patched, which in turn is endocytosed, thereby degrading the ligand. In the case of retinoic acid, its signal induces the expression of the retinoic acid-degrading enzyme Cyp26a1. Thus, the degradation of these morphogens is enhanced in those spatial regions of high morphogen activity. This kind of feedback between morphogen signalling and degradation (and hence, formation) can be modelled mathematically by setting the morphogen degradation as nonlinear (at least close to the source) (Eldar *et al*, 2003). The steady-state profile of a dynamic involving diffusion and nonlinear degradation can be obtained analytically and corresponds to a power-law shape (it decays more abruptly close to the source and less markedly on the tails than an exponential profile) (Eldar *et al*, 2003). But is this feedback relevant? Mathematical analysis of the gradient profiles when gene dosage is increased reveals that this differential degradation confers robustness to these changes (Eldar *et al*, 2003), indicating that this robustness may be a desired property of the morphogen gradient.

The transport of a morphogen

The concept of morphogen gradients is tightly related to long-range signalling. How can molecules span over large spatial regions to elicit direct responses? According to the values known for the diffusion rates of molecules, Francis Crick proposed that diffusion enables the formation of gradients over fields of 50 cells within a scale of a few hours (Crick, 1970). Since then, diffusion has taken the leading role as the transport mechanism for gradient formation. At present, diffusion is commonly named restricted or effective diffusion, to emphasize that the diffusion rate values in the extracellular medium are much smaller than those measured in aqueous media (Tabata and Takei, 2004; Strigini, 2005; Kicheva *et al*, 2007). The difference in such rates is thought to arise partially from the properties of the extracellular medium, a crowded environment with non-uniform matrix geometries and molecular distributions that interact with the morphogen. In addition, the effective diffusion can involve other non-directional random transports. For instance, the recently inferred that effective diffusion rate of Dpp, $D=0.1\,\mu m^2/s$, is much (three orders of magnitude) smaller than what it would be expected according to its size when diffusing freely in water (Kicheva *et al*, 2007). Note that the procedure involved in inferring this value took all kinds of Dpp transport as a single diffusive-like motion, as described above. Therefore, this rate corresponds to an effective motion in which other non-directional random transports can be involved, which potentially may strongly slow down the dynamics.

Diffusion arises from the random motion of molecules. Molecules perform a kind of random walk-like motion going in all, even opposite, directions. Thus, the mean displacement of molecules does not increase linearly with time, as in ballistic motion, but much more slowly, as the root square of time. This pure diffusion is not the only passive random motion molecules can trace within a biological medium. Indeed, in prokaryotes, large biological molecules such as mRNAs have been shown to perform an intracellular random motion slower than diffusion and named subdiffusion, that is, the mean displacement of mRNA molecules increases over time much more slowly as $\sqrt{t^\alpha}$ with $\alpha < 1$ (t stands for the time) (Golding and Cox, 2006). Likely elements that underlie such behaviour are the random trapping and binding of the mRNA molecules with other molecules inside the crowded intracellular environment and, accordingly, smaller molecules such as proteins are expected to be less influenced (Elowitz *et al*, 1999; Golding and Cox, 2006). In addition, cytoskeletal dynamics in eukaryotic cells can elicit fast random molecular motions, in between diffusion and ballistic movement, called super-diffusive motions (Lau *et al*, 2003), that is, the mean squared displacement follows over time a power-law dynamic with an exponent greater than 1. Theoretical analysis evaluating the effect of subdiffusive random motions on the formation of gradients has started (Hornung *et al*, 2005). Future work is thus expected to elucidate how the random motion of proteins occurs extracellularly and within cells to form a morphogen gradient and how the gradient profile and dynamics depend on this motion.

In the last decade, driven by novel molecular data, new biological transport mechanisms for secreted morphogens that involve active processes have been proposed (for reviews, see Zhu and Scott, 2004; Strigini, 2005; Figure 3A). Vesicle-mediated transport mechanisms that can take place along the extracellular space have been shown (Greco *et al*, 2001; Panáková *et al*, 2005; Tanaka *et al*, 2005). Direct long-range interactions through long cellular protrusions have been suggested as well (Ramírez-Weber and Kornberg, 1999). In addition, transport through cells mediated by cycles of endocytosis and exocytosis (named 'transcytosis') has been proposed (reviewed by Vincent and Dubois, 2002; Gonzalez-Gaitan, 2003). Data on mosaic experiments in the fly's wing, which set a patch of cells with impaired endocytosis near the Dpp morphogen source, raised the question of whether diffusion was the main mechanism of Dpp transport (Entchev *et al*, 2000). During gradient formation, the amount of Dpp morphogen decayed strongly behind the clone of cells (showing a so-called 'shadow'), which suggested that the transport of Dpp requires endocytosis to reach those cells (Entchev *et al*, 2000). However, a mathematical and numerical analysis challenged this view (Lander *et al*, 2002). In the model that was formulated, Dpp transport was driven just by diffusion. Internalization and recycling of the free ligand and of bound receptors was considered, as well as degradation of these molecules inside cells. Impaired endocytosis was modelled as a reduction of the internalization rate and an increase of cell surface receptors. In this scenario, Dpp became trapped through its binding with the high amount of cell surface receptors and a shadow appeared behind the clone. Therefore, the appearance of 'shadows' could not be used to exclude diffusion as the transport mechanism (Lander *et al*, 2002). However, despite exhibiting a shadow, the morphogen

profile did not agree completely with the experimental data (Gonzalez-Gaitan, 2003). Another theoretical analysis reformulated the same model, by extending it to two dimensions and setting a different parameter-dependent source of receptors and different boundary conditions, to name some of the changes. Impaired endocytosis was modelled as a reduction of the internalization rates, and the results showed that a natural strong and rapid accumulation of receptors occurred within the clone, which was essential to cause a shadow (Kruse *et al*, 2004). However, no such increase could be found experimentally, nor was the ligand profile totally consistent with mosaic data, pinpointing that diffusion could not be the single mechanism of Dpp transport (Kruse *et al*, 2004). Recent new theoretical modelling that takes into account Dpp transport through both transcytosis and diffusion at the scale of each cell has been able to obtain more proper ligand profiles as observed in mosaic experiments, even when the total amount of cell surface receptors is constant, supporting transcytosis as a mechanism for Dpp transport (Bollenbach *et al*, 2007). In addition to their relevance in addressing the issue of how Dpp is transported, all these studies exemplify how many challenges we also face from a theoretical point of view when trying to reject the plausibility of a mechanism.

The study of morphogen gradients has focused on secreted molecules, partially because these molecules can move extracellularly over large distances. However, molecular gradients along a cellular tissue can arise without requiring any dynamics on the extracellular space (Figure 3A). On the one hand, transport from cell to cell through gap junctions can occur (Esser *et al*, 2006). On the other hand, cells can be the transport vehicle of the molecule (Lecuit and Cohen, 1998; Tabata, 2001; Teleman *et al*, 2001). In the last years, experimental and theoretical evidence in favour of cellular-based transport mechanisms has been shown (Pfeiffer *et al*, 2000; Gaunt *et al*, 2003; Dubrulle and Pourquié, 2004; Ibañes *et al*, 2006). These kinds of transport enable the formation of gradients of non-secreted molecules. Two mechanisms, which can both take place for the same molecular gradient, have risen. In both cases, the source corresponds to a spatial region where cells divide and have the ability to produce the molecular component (e.g. the mRNA). Thus, when cells become placed outside this region, they cease to produce the molecule. If over time cells move or become displaced further away from the source while degrading their molecular content, a spatial gradient is formed (Gaunt *et al*, 2003; Dubrulle and Pourquié, 2004; Ibañes *et al*, 2006). In addition, molecular gradients can also be formed by the dilution of the molecular content on cells that continuously divide and become displaced away from the source, a mechanism termed cell-lineage transport (Ibañes *et al*, 2006).

Gradients of non-secreted molecules can in turn create graded distributions of secreted factors and other kinds of molecules. As indicated, gradients of mRNA provide a graded source for protein translation, which elicits a protein gradient (Dubrulle and Pourquié, 2004; Ibañes *et al*, 2006). In addition, gradients of non-secreted molecules can potentially convert a molecular uniform distribution into a morphogen or signalling gradient, by modulating its degradation or its transduction, respectively, on each cell. For instance, if the non-secreted molecule inhibits morphogen degradation, the morphogen

will be less degraded in cells close to the source of the non-secreted molecule than in more distant cells. Thus, differential degradation along a field of cells could induce a morphogen gradient. Until now, differential degradation mediated by gradients of secreted molecules has been shown to shape and stabilize morphogen gradients. This is the case of the anterior-to-posterior gradient of retinoic acid in the developing nervous system of zebrafish embryos (White *et al*, 2007), which is shaped by a parallel gradient of the secreted factor Fgf8 that suppresses the degradation of retinoic acid by inhibiting the expression of the degrading enzyme Cyp26a1.

The formation of a single morphogen gradient can be driven by several of the transport mechanisms described so far, altogether enhancing the long-range transport of the morphogen. For instance, the FGF8 protein gradient from the tail bud to more anterior regions in vertebrate embryos might be driven by diffusion as well as by cell-based transport mechanisms. This is a very complex system that will require both challenging experimental and theoretical strategies to be fully characterized. As diffusion sets a much faster spatiotemporal dynamic than cell division in the tail bud region, increasing the degradation rate of Fgf8 to values in which tissue growth cannot drive protein transport could provide information on the range and rate of Fgf8 diffusion. Thus, theoretical predictions on the spatial range of the gradient based on diffusive transport alone could be compared with *in vivo* data. In addition, setting a framework that couples both transport mechanisms at the cellular level (i.e. at this scale, diffusive transport might be seen as a slave dynamic that quickly adapts to perturbations set by proliferating cells) could evaluate how single cells sense the gradient and act on it.

Gradient dynamics

Much work on morphogen gradients assumes that cells sense and interpret a steady morphogen concentration. Accordingly, focus has been set on modelling the formation of steady-state gradients. By analytically and numerically solving the gradient dynamics and the steady-state solution, it can be seen that the transient and steady-state gradients depend distinctly on the parameter values that characterize the transport, the degradation and the source rates (Figure 1C and D) and thus will respond to changes in a different manner (Bergmann *et al*, 2007; Lander, 2007). The different response transient and steady-state gradients will be relevant if we take into account that it is not always easy to know whether a morphogen gradient has reached its steady state *in vivo* (Bergmann *et al*, 2007, 2008; Gregor *et al*, 2007b; Bialek *et al*, 2008).

As ultimately cells sense the morphogen and interpret it accordingly, it is interesting to know how cells see the gradient over time. In addition, not all cells may respond simultaneously to the gradient, but alternatively each cell (or groups of cells) may respond to the gradient at a different time, as it has been described for BMP signalling (Tucker *et al*, 2008). While a gradient driven by diffusion or other molecular transport mechanism is being formed in a static field of cells, the cells are exposed to increasing levels of morphogen over time. Cells located close to the source are the ones to first sense the morphogen and to experience higher morphogen levels

than cells located at farther distances. Once the steady state has been reached, cells sense a constant amount of morphogen, which depends on where the cell is located. But even if the gradient is in a steady state, its activity can be dynamical and transient. This is the case of the activity of Sonic hedgehog (a vertebrate homologue of invertebrate hedgehog) in vertebrate neural cells, which lasts a time period proportional to the amount of morphogen (Dessaud *et al*, 2007).

Gradients driven by cell-based transport involve a dynamic field of cells. In this case, the molecular content inside cells does not reach a steady state and cells sense a decreasing molecular amount over time, which is related to their increasing distance from the source (Ibañes *et al*, 2006). Therefore, the way cells sense the gradient and thus can subsequently interpret it strongly depends on the mechanism of gradient formation and signalling.

Gradient interpretation is not just the final step

Three main questions are involved in gradient interpretation: which is the graded information that is interpreted? How does this interpretation occur? And what does this graded information specify? Over the last few decades, several groups have started addressing these questions, uncovering further complexities involved in morphogen gradients.

The study of different morphogens has shown that the graded information (or signal) that is interpreted may depend on the specific morphogen gradient. Thus, the graded signal can be the steady-state amount of morphogen around a cell, which might be measured by the number of bound receptors or, alternatively, by the ratio of bound to unbound receptors (Dyson and Gurdon, 1998; Gurdon and Bourillot, 2001; Casali and Struhl, 2004). It could also be the amount of morphogen in a transient dynamic state (Bergmann *et al*, 2007). Another option is that the graded signal that is interpreted is not the level of morphogen but instead it is the steepness of the gradient (Lawrence, 2001; Rogulja and Irvine, 2005). Alternatively, the signal that is interpreted could be the total amount of morphogen cells have been exposed to over time (Ahn and Joyner, 2004; Harfe *et al*, 2004; McGlinn and Tabin, 2006; Tarchini and Duboule, 2006; Tabin and Wolpert, 2007). Moreover, the morphogen level could be transduced into a graded time period of activity that is interpreted (Dessaud *et al*, 2007).

Experimental evidence indicates that morphogen gradients can direct more than two different cell fates. Commonly, the specification of distinct fates has been addressed in terms of the induction of downstream genes (for review, see Ashe and Briscoe, 2006). Accordingly, distinct cellular responses are characterized by which targets are active (Figures 1A and 4D). The graded signal coming from the morphogen is thus converted into roughly binary responses of each target, defining sharp response borders (Figure 4B and D). Different
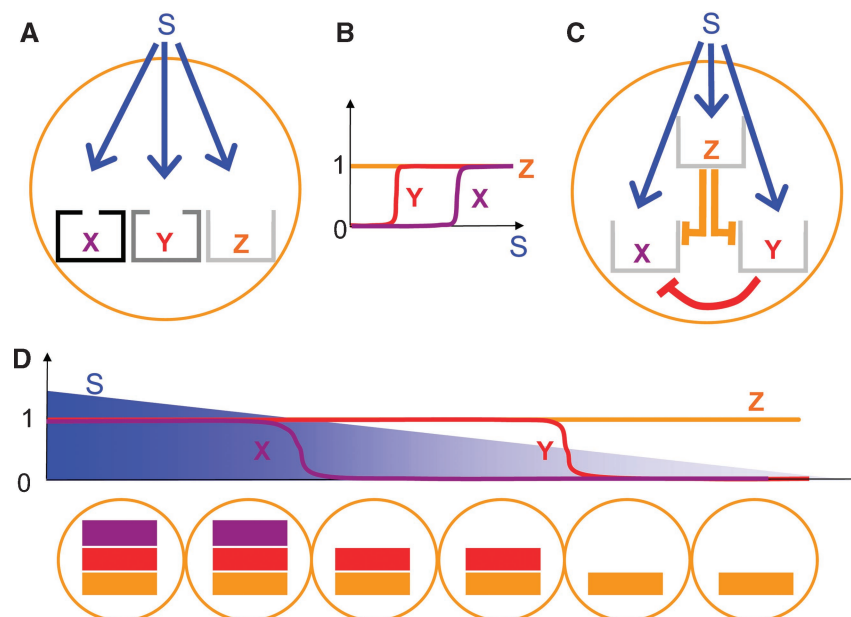
Figure 4 Morphogen gradient interpretation. (**A**) The morphogen gradient elicits a signal (S, in blue) to which a cell (orange circle) responds. The signal induces (blue arrows) the expression of targets X, Y and Z. These targets have different sensitivity (denoted by open squared boxes) to the same signal S. X is weakly sensitive to S, Y is mildly sensitive and Z is very sensitive. (**B**) Binary response of target genes X, Y and Z to signal S. Low levels of S activate only Z, medium levels activate both Z and Y, and high levels activate all targets. (**C**) The signal induces the expression of targets X, Y and Z, which here have the same sensitivity but interact with each other. An example of plausible cell-autonomous interactions is depicted, in which Z represses both Y and X, and Y represses X (repression is shown by curves with line-end; arrows indicate induction). In this case, to elicit different responses along a gradient, different sensitivities are not required, but could also be participating. As X is repressed by Y and Z, the overall signal it perceives is smaller than the signal Y perceives, which, in turn, is smaller than the signal Z perceives. Thus, the binary response of the target genes to different values of signal S is also shown in (B). (**D**) X, Y and Z binary response (lines) to a graded signal (S, blue triangle) along a field of cells (orange circles). Three different spatial regions and fates are induced, which are characterized by those genes that are expressed. Expression inside cells is denoted by a coloured rectangle (violet for X, red for Y and orange for Z).

mechanisms ranging from positive feedback, cooperativity and zero-order ultrasensitivity have been shown to convert a graded signal into a binary response (for reviews, see Ferrell, 2002; Ashe and Briscoe, 2006). Theoretical approaches have been important to propose and characterize these mechanisms for switch-like behaviour by analysing the steady states of a specific cell-autonomous dynamic under an external input stimulus (Box 3).

Box 3 How to infer the mechanism of gradient interpretation? An example of a procedure

To address gradient interpretation, the morphogen gradient or its targets need to be altered and the shifts on cell fate and on downstream targets that are elicited accordingly need to be measured. The extent of the shift (both in space and time) will depend crucially on the mechanism of gradient interpretation taking place. Thus, data on the actual shifts can be used to potentially discard scenarios of gradient interpretation. An illustration of these concepts is provided by the study of how a continuous gradient can be converted into sharp developmental domains in *Drosophila* embryos (Melen *et al*, 2005).

The ventral ectoderm of *Drosophila* embryos is patterned by a gradient of the secreted ligand Spitz, a TGF-α homologue. Spitz is secreted by a single row of glial cells at the midline. On binding to epidermal growth factor receptor (EGFR), it activates mitogen-activated protein kinase (MAPK), inducing a gradient of EGFR activation and MAPK over five rows of cells on either side of the midline. MAPK in turn regulates several target genes. Specifically, it controls the degradation of the transcriptional repressor Yan. As a result, Yan protein is absent from the two cell rows that are closest to the midline and it is found at a uniform level on the remaining cell rows. Therefore, the gradient of MAPK is converted into a binary response of Yan protein levels (Melen *et al*, 2005). To decipher how this response is elicited, Melen *et al* (2005) constructed a mathematical model that could analyse three mechanisms of sharp graded-to-binary conversion: cooperativity, positive feedback and zero-order ultrasensitivity (indeed, the model studied first-order conversion as well, which elicits more gradual responses and which we do not detail herein for simplicity). In the model, the amount of MAPK is the signal that is interpreted and it triggers a cell-autonomous dynamic that facilitates Yan degradation through its MAPK-mediated phosphorylation. By numerically finding the steady state of Yan expression in a single cell for different levels of MAPK, it was found that cooperativity (driven by multiple MAPK bindings), positive feedback (elicited when Yan dephosphorylation rate decreases with the level of phosphorylated Yan) and zero-order ultrasensitivity (the levels of MAPK and phosphatase enzyme are limiting whereas the substrate Yan is in excess) all elicit a sharp binary response, and a similar threshold of MAPK activity can be defined below which Yan is expressed. Therefore, by looking just at the wild-type Yan expression, none of the three mechanisms could be discarded and all seemed plausible. However, numerical analysis of the dynamics and steady state of Yan levels showed that responses to Yan overexpression are specific for each mechanism. Thus, when Yan is overexpressed, a shift towards the midline of steady-state Yan expression occurs if positive feedback is controlling the conversion. In contrast, no shifts are elicited when cooperative and zero-order ultrasensitivity mechanisms do the interpretation. In addition, the time to reach the steady state increases strongly, such that transient ectopic Yan expression in all cells should be noticeable only if zero-order ultrasensitivity is driving the process. Therefore, these analyses revealed that the actual mechanism of gradient interpretation could be deciphered if Yan was ectopically expressed and the transient and steady state patterns of Yan expression were measured. *In vivo* ectopic expression of Yan in *Drosophila* embryos showed no shift of Yan expression at long times (discarding positive feedback), and a long transient distribution of exogenous Yan. Therefore, these data on spatial and temporal shifts of Yan expression pointed to zero-order ultrasensitivity to be the mechanism converting MAPK graded signal into a Yan degradation binary response (Melen *et al*, 2005).

How does the morphogen gradient specify several distinct fates? On the one hand, the targets of the morphogen signal can be characterized by different levels of sensitivity (Figure 4A). This sensitivity can correspond to the affinities of the target genes to morphogen signal-binding sites. Each target will respond above a different threshold signal, which will depend on the affinity of the morphogen-binding site (i.e. those targets that exhibit low affinity will respond to only high levels of the signal, whereas those with high affinity will respond to lower levels of the signal; see Figure 4B). Thus, the level of morphogen signal will select which targets are induced, and a pattern over space of different activated targets will be elicited (Figure 4D). On the other hand, the morphogen signal can similarly activate or repress several targets, which, as a result of their interaction within a network, respond distinctly to the same signal (Figure 4B and C). Accordingly, for a graded signal over space, a pattern of different active targets will arise (Figure 4D). In this case, although the sensitivity of the targets might be the same, the response will differ depending on the amount of signal. Note that a huge landscape of different network topologies and dynamics can be envisaged that could elicit many diverse patterns. Importantly, the two strategies being described can be acting at the same time on a single morphogen to direct a response. Indeed, both mechanisms have been reported for the Bicoid gradient. The number and affinity of Bicoid-binding sites provide a different level of sensitivity to the Bicoid signal (Driever *et al*, 1989c; Struhl *et al*, 1989; Gao *et al*, 1996). In addition, downstream target gap genes, activated by Bicoid, repress each other and thus also interpret the gradient through their interaction (Jaeger *et al*, 2004; Jaeger and Reinitz, 2006; Bergmann *et al*, 2007). However, in addition, a bioinformatic analysis has found out that the combination of several additional activators that bind the promoter regions of Bicoid target genes can be relevant to control and specify the Bicoid gradient interpretation (Ochoa-Espinosa *et al*, 2005).

Distinct patterns of gene expression between cells are expected to elicit ultimately different cellular behaviours. Specifically, the Dpp gradient in the wing of *Drosophila* embryos has been shown to control cell proliferation (Rogulja and Irvine, 2005). In addition, the FGF8 gradient in the presomitic mesoderm of chick embryos is translated into a gradient of extracellular signal-regulated kinase (ERK), which promotes cell migration (Delfini *et al*, 2005). Can this induced cell behaviour in turn alter the morphogen gradient, setting a feedback between gradient formation and interpretation? Potentially yes, as cell dynamics can shape morphogen gradients (Dubrulle and Pourquié, 2004; Ibañes *et al*, 2006). Indeed, cell dynamics are essential to create the mRNA *fgf8* gradient (Dubrulle and Pourquié, 2004). Thus, these cell dynamics can have an important role in shaping the protein and ERK signalling gradient as well. The relevance of such feedback, according to the timescale of gradient interpretation, cellular response and gradient formation, will require a careful evaluation aided by theoretical approaches. Moreover, molecular feedbacks between gradient signalling and formation (such as those eliciting enhanced degradation, as previously discussed) have been uncovered (Lander, 2007), which stress, as well, the importance of evaluating the process of formation and interpretation altogether as a whole system.

Future perspectives: a systems biology approach for morphogen gradients

Morphogen gradients have been an extremely useful framework to characterize pattern formation processes in developing embryos. Despite their apparent simplicity, novel data on morphogen gradients are stressing and expanding the complexities that this framework involves. Thus, morphogen gradients exemplify most of the complexities we have to tackle when studying embryonic development: the interplay between several and different levels of organization, time and spatial scales and components. Morphogen gradients pose two advantages, that is, the thorough knowledge we have acquired in the last decades on this topic and the additional knowledge we gain each time we use theoretical and computational strategies combined with experimental approaches to decipher their features.

New data have shown cell-based mechanisms for the transport of molecules that allow the formation of gradients of non-secreted molecules. If such gradients are shown to shape graded information to which cells respond, morphogens should be extended to include non-secreted molecules. In addition, these and other data have highlighted that knowing the dynamics of gradients, and not only their steady state, is becoming increasingly important. At present, we still know very little about how the dynamics of gradients participate in the overall process of gradient interpretation. To shed some light on this issue, mathematical approaches can be extremely useful by predicting the kind of response we might expect.

In most cases, the shape and dynamics of morphogen gradient formation are analysed independent of gradient interpretation. Thus, gradient interpretation has been commonly neglected when studying gradient formation. However, some of the findings we have highlighted herein emphasize a very important issue that has been largely avoided: the gradient can depend on the response it elicits. As the response is directed by the gradient, a feedback between gradient and response can be present. At the molecular level, such feedback has already been taken into account: morphogen signalling can feedback to receptor or ligand production, modifying the profile of the gradient (Lander, 2007). However, such feedback does not necessarily occur just at the molecular level but can also involve the cell dynamics. We have seen that morphogen gradients can induce changes in the dynamics of cells, activating their proliferative and migratory state (Delfini et al, 2005; Rogulja and Irvine, 2005). As cell proliferation and spatiotemporal cell displacement can shape a gradient (Ibañes et al, 2006), such a cellular response can modify the gradient in return. Thus, as the responses at both the molecular and cellular levels can shape the morphogen gradient, it becomes necessary to study gradient formation and interpretation processes together (Figure 5).

Therefore, understanding pattern formation through morphogen gradients can require integrative approaches that take both gradient formation and interpretation into account in a common framework. Hence, we suggest system-level perspectives on morphogen gradients that address the problem of pattern formation from gradient formation to gradient interpretation and vice versa. Moreover, by defining the morphogen system as the molecules forming the gradient, the graded
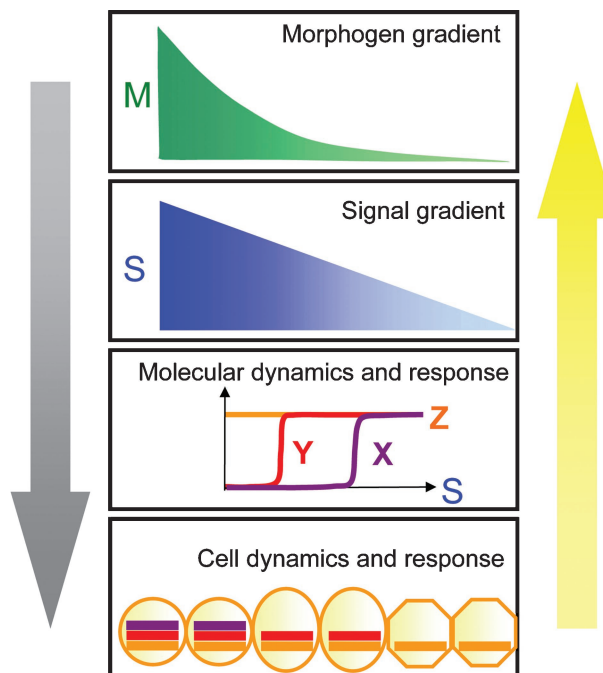
Figure 5 A systems biology approach to morphogen gradients. Morphogen gradient formation and interpretation involve several processes depicted from top to bottom. The morphogen gradient induces (grey arrow) a graded signal (in green). This signal does not necessarily exhibit the same gradient profile as the morphogen gradient. The signal elicits molecular and cell response dynamics (grey arrow). However, there are also feedback interactions: the morphogen gradient and the signal gradient depend on the molecular and cellular dynamics they induce (yellow arrow).

signal and the interpretation dynamics, new perspectives will be gained. Issues such as finding those reliable dynamics of the morphogen system, and how this reliability and performance is achieved can uncover vital insights (Eldar et al, 2003; Lander, 2007). By implicitly neglecting such feedback, we reduce the range of possible designs enabling morphogen reliability: the morphogen gradient itself is very reliable and such robustness is preserved during gradient interpretation; alternatively, the process of gradient interpretation is responsible for setting a reliable response from a variable graded input. Yet, a system approach will broaden the scope and another plausible answer could arise: reliability depends on the interaction between formation and interpretation dynamics.

Acknowledgements

References

Aegerter-Wilmsen T, Aegerter CM, Bisseling T (2005) Model for the robust establishment of precise proportions in the early *Drosophila* embryo. *J Theor Biol* **234:** 13–19

Affolter M, Basler K (2007) The Decapentaplegic morphogen gradient: from pattern formation to growth regulation. *Nat Rev Genet* **8:** 663–674

Ahn S, Joyner AL (2004) Dynamic changes in the response of cells to positive hedgehog signaling during mouse limb patterning. *Cell* **118:** 505–516

Ashe H, Briscoe J (2006) The interpretation of morphogen gradients. *Development* **133:** 385–394

Ashe HL, Mannervik M, Levine M (2000) Dpp signaling thresholds in the dorsal ectoderm of the *Drosophila* embryo. *Development* **127:** 3305–3312

Bergmann S, Sandler O, Sberro H, Shnider S, Schejter E, Shilo B-Z, Barkai N (2007) Pre-steady-state decoding of the bicoid morphogen gradient. *PLoS Biol* **5:** e46

Bergmann S, Tamari Z, Schejter E, Shilo BZ, Barkai N (2008) Re-examining the stability of the bicoid morphogen gradient. *Cell* **132:** 15–17

Bialek W, Gregor T, Tank DW, Wieschaus EF (2008) Response: can we fit all of the data? *Cell* **132:** 17–18

Bollenbach T, Kruse K, Pantazis P, González-Gaitán M, Jülicher F (2005) Robust formation of morphogen gradients. *Phys Rev Lett* **94:** 018103

Bollenbach T, Kruse K, Pantazis P, González-Gaitán M, Jülicher F (2007) Morphogen transport in epithelia. *Phys Rev E Stat Nonlin Soft Matter Phys* **75:** 011901

Casali A, Struhl G (2004) Reading the Hedgehog morphogen gradient by measuring the ratio of bound to unbound Patched protein. *Nature* **431:** 76–80

Chen Y, Schier AF (2001) The zebrafish Nodal signal Squint functions as a morphogen. *Nature* **411:** 607–610

Crick F (1970) Diffusion in embryogenesis. *Nature* **225:** 420–422

Delfini MC, Dubrulle J, Malapert P, Chal J, Pourquie O (2005) Control of the segmentation process by graded MAPK/ERK activation in the chick embryo. *Proc Natl Acad Sci USA* **102:** 11343–11348

Dessaud E, Yang LL, Hill K, Cox B, Ulloa F, Ribeiro A, Mynett A, Novitch BG, Briscoe J (2007) Interpretation of the sonic hedgehog morphogen gradient by a temporal adaptation mechanism. *Nature* **450:** 717–720

Dorfman R, Shilo BZ (2001) Biphasic activation of the BMP pathway patterns the *Drosophila* embryonic dorsal region. *Development* **128:** 965–972

Driever W, Ma J, Nüsslein-Volhard C, Ptashne M (1989a) Rescue of bicoid mutant *Drosophila* embryos by bicoid fusion proteins containing heterologous activating sequences. *Nature* **342:** 149–154

Driever W, Nüsslein-Volhard C (1988a) The bicoid protein determines position in the *Drosophila* embryo in a concentration-dependent manner. *Cell* **54:** 95–104

Driever W, Nüsslein-Volhard C (1988b) A gradient of bicoid protein in *Drosophila* embryos. *Cell* **54:** 83–93

Driever W, Nüsslein-Volhard C (1989b) The bicoid protein is a positive regulator of hunchback transcription in the early *Drosophila* embryo. *Nature* **337:** 138–143

Driever W, Thoma G, Nüsslein-Volhard C (1989c) Determination of spatial domains of zygotic gene expression in the *Drosophila* embryo by the affinity of binding sites for the bicoid morphogen. *Nature* **340:** 363–367

Dubrulle J, Pourquié O (2004) fgf8 mRNA decay establishes a gradient that couples axial elongation to patterning in the vertebrate embryo. *Nature* **427:** 419–422

Dyson S, Gurdon JB (1998) The interpretation of position in a morphogen gradient as revealed by occupancy of activin receptors. *Cell* **93:** 557–568

Eldar A, Dorfman R, Weiss D, Ashe H, Shilo BZ, Barkai N (2002) Robustness of the BMP morphogen gradient in *Drosophila* embryonic patterning. *Nature* **419:** 304–308

Eldar A, Rosin D, Shilo BZ, Barkai N (2003) Self-enhanced ligand degradation underlies robustness of morphogen gradients. *Dev Cell* **5:** 635–646

Elowitz MB, Surette MG, Wolf PE, Stock JB, Leibler S (1999) Protein mobility in the cytoplasm of *Escherichia coli*. *J Bacteriol* **181:** 197–203

England JL, Cardy J (2005) Morphogen gradient from a noisy source. *Phys Rev Lett* **94:** 078101

Entchev EV, Schwabedissen A, González-Gaitán M (2000) Gradient formation of the TGF-beta homolog Dpp. *Cell* **103:** 981–991

Ephrussi A, Johnston D (2004) Seeing is believing: the bicoid morphogen gradient matures. *Cell* **116:** 143–152

Esser AT, Smith KC, Weaver JC, Levin M (2006) Mathematical model of morphogen electrophoresis through gap junctions. *Dev Dyn* **235:** 2144–2159

Ferguson EL, Anderson KV (1992) Decapentaplegic acts as a morphogen to organize dorsal–ventral pattern in the *Drosophila* embryo. *Cell* **71:** 451–461

Ferrell Jr JE (2002) Self-perpetuating states in signal transduction: positive feedback, double-negative feedback and bistability. *Curr Opin Cell Biol* **14:** 140–148

Gao Q, Wang Y, Finkelstein R (1996) Orthodenticle regulation during embryonic head development in *Drosophila*. *Mech Dev* **56:** 3–15

Gaunt SJ, Drage D, Cockley A (2003) Vertebrate caudal gene expression gradients investigated by use of chick cdx-A/lacZ and mouse cdx-1/lacZ reporters in transgenic mouse embryos: evidence for an intron enhancer. *Mech Dev* **120:** 573–586

Golding I, Cox EC (2006) Protein synthesis molecule by molecule. *Genome Biol* **7:** 221

Gonzalez-Gaitan M (2003) Endocytic trafficking during *Drosophila* development. *Mech Dev* **120:** 1265–1282

Greco V, Hannus M, Eaton S (2001) Argosomes: a potential vehicle for the spread of morphogens through epithelia. *Cell* **106:** 633–645

Green J (2002) Morphogen gradients, positional information, and *Xenopus*: interplay of theory and experiment. *Dev Dyn* **225:** 392–408

Gregor T, Bialek W, de Ruyter van Steveninck RR, Tank DW, Wieschaus EF (2005) Diffusion and scaling during early embryonic pattern formation. *Proc Natl Acad Sci USA* **102:** 18403–18407

Gregor T, Tank DW, Wieschaus EF, Bialek W (2007a) Probing the limits to positional information. *Cell* **130:** 153–164

Gregor T, Wieschaus EF, McGregor AP, Bialek W, Tank DW (2007b) Stability and nuclear dynamics of the bicoid morphogen gradient. *Cell* **130:** 141–152

Gurdon JB, Bourillot PY (2001) Morphogen gradient interpretation. *Nature* **413:** 797–803

Gurdon JB, Harger P, Mitchell A, Lemaire P (1994) Activin signalling and response to a morphogen gradient. *Nature* **371:** 487–492

Harfe BD, Scherz PJ, Nissim S, Tian H, McMahon AP, Tabin CJ (2004) Evidence for an expansion-based temporal Shh gradient in specifying vertebrate digit identities. *Cell* **118:** 517–528

Hornung G, Berkowitz B, Barkai N (2005) Morphogen gradient formation in a complex environment: an anomalous diffusion model. *Phys Rev E Stat Nonlin Soft Matter Phys* **72:** 041916

Houchmandzadeh B, Wieschaus E, Leibler S (2002) Establishment of developmental precision and proportions in the early *Drosophila* embryo. *Nature* **415:** 798–802

Houchmandzadeh B, Wieschaus E, Leibler S (2005) Precise domain specification in the developing *Drosophila* embryo. *Phys Rev E Stat Nonlin Soft Matter Phys* **72:** 061920

Howard M, ten Wolde PR (2005) Finding the center reliably: robust patterns of developmental gene expression. *Phys Rev Lett* **95:** 208103

Ibañes M, Kawakami Y, Rasskin-Gutman D, Izpisua-Belmonte JC (2006) Cell lineage transport: a mechanism for molecular gradient formation. *Mol Syst Biol* **2:** 57

Izpisúa-Belmonte JC, Tickle C, Dollé P, Wolpert L, Duboule D (1991) Expression of the homeobox Hox-4 genes and the specification of position in chick wing development. *Nature* **350:** 585–589

Jaeger J, Reinitz J (2006) On the dynamic nature of positional information. *BioEssays* **28:** 1102–1111

Jaeger J, Surkova S, Blagov M, Janssens H, Kosman D, Kozlov KN, Manu, Myasnikova E, Vanario-Alonso CE, Samsonova M, Sharp DH, Reinitz J (2004) Dynamic control of positional information in the early *Drosophila* embryo. *Nature* **430:** 368–371

Kerszberg M, Wolpert L (1998) Mechanisms for positional signalling by morphogen transport: a theoretical study. *J Theor Biol* **191:** 103–114

Kicheva A, Pantazis P, Bollenbach T, Kalaidzidis Y, Bittig T, Jülicher F, González-Gaitán M (2007) Kinetics of morphogen gradient formation. *Science* **315:** 521–525

Kruse K, Pantazis P, Bollenbach T, Jülicher F, González-Gaitán M (2004) Dpp gradient formation by dynamin-dependent endocytosis: receptor trafficking and the diffusion model. *Development* **131:** 4843–4856

Lander A (2007) Morpheus unbound: reimagining the morphogen gradient. *Cell* **128:** 245–256

Lander AD, Nie Q, Wan FY (2002) Do morphogen gradients arise by diffusion? *Dev Cell* **2:** 785–796

Lander AD, Nie Q, Wan FY (2007) Membrane-associated non-receptors and morphogen gradients. *Bull Math Biol* **69:** 33–54

Lau AW, Hoffman BD, Davies A, Crocker JC, Lubensky TC (2003) Microrheology, stress fluctuations, and active behavior of living cells. *Phys Rev Lett* **91:** 198101

Lawrence PA (2001) Morphogens: how big is the big picture? *Nat Cell Biol* **3:** E151–E154

Lecuit T, Cohen SM (1998) Dpp receptor levels contribute to shaping the Dpp morphogen gradient in the *Drosophila* wing imaginal disc. *Development* **125:** 4901–4907

Martinez Arias A (2003) Wnts as morphogens? The view from the wing of *Drosophila*. *Nat Rev Mol Cell Biol* **4:** 321–325

McDowell N, Gurdon JB, Grainger DJ (2001) Formation of a functional morphogen gradient by a passive process in tissue from the early *Xenopus* embryo. *Int J Dev Biol* **45:** 199–207

McGlinn E, Tabin CJ (2006) Mechanistic insight into how Shh patterns the vertebrate limb. *Curr Opin Genet Dev* **16:** 426–432

McHale P, Rappel WJ, Levine H (2006) Embryonic pattern scaling achieved by oppositely directed morphogen gradients. *Phys Biol* **3:** 107–120

Melen GJ, Levy S, Barkai N, Shilo BZ (2005) Threshold responses to morphogen gradients by zero-order ultrasensitivity. *Mol Syst Biol* **1:** 2005.0028

Mizutani CM, Nie Q, Wan FY, Zhang YT, Vilmos P, Sousa-Neves R, Bier E, Marsh JL, Lander AD (2005) Formation of the BMP activity gradient in the *Drosophila* embryo. *Dev Cell* **8:** 915–924

Morgan TH (1901) *Regeneration*. New York: MacMillan

Nellen D, Burke R, Struhl G, Basler K (1996) Direct and long-range action of a DPP morphogen gradient. *Cell* **85:** 357–368

Ochoa-Espinosa A, Yucel G, Kaplan L, Pare A, Pura N, Oberstein A, Papatsenko D, Small S (2005) The role of binding site cluster strength in Bicoid-dependent patterning in *Drosophila*. *Proc Natl Acad Sci USA* **102:** 4960–4965

Panáková D, Sprong H, Marois E, Thiele C, Eaton S (2005) Lipoprotein particles are required for Hedgehog and Wingless signalling. *Nature* **435:** 58–65

Pfeiffer S, Alexandre C, Calleja M, Vincent JP (2000) The progeny of wingless-expressing cells deliver the signal at a distance in *Drosophila* embryos. *Curr Biol* **10:** 321–324

Ramírez-Weber FA, Kornberg TB (1999) Cytonemes: cellular processes that project to the principal signaling center in *Drosophila* imaginal discs. *Cell* **97:** 599–607

Rivera-Pomar R, Jäckle H (1996) From gradients to stripes in *Drosophila* embryogenesis: filling in the gaps. *Trends Genet* **12:** 478–483

Rogulja D, Irvine KD (2005) Regulation of cell proliferation by a morphogen gradient. *Cell* **123:** 449–461

Schier AF, Talbot WS (2005) Molecular genetics of axis formation in zebrafish. *Annu Rev Genet* **39:** 561–613

Shimizu K, Gurdon JB (1999) A quantitative analysis of signal transduction from activin receptor to nucleus and its relevance to morphogen gradient interpretation. *Proc Natl Acad Sci USA* **96:** 6791–6796

Shimmi O, Umulis D, Othmer H, O'Connor MB (2005) Facilitated transport of a Dpp/Scw heterodimer by Sog/Tsg leads to robust patterning of the *Drosophila* blastoderm embryo. *Cell* **120:** 873–886

Simeoni I, Gurdon JB (2007) Interpretation of BMP signaling in early *Xenopus* development. *Dev Biol* **308:** 82–92

St Johnston D, Nüsslein-Volhard C (1992) The origin of pattern and polarity in the *Drosophila* embryo. *Cell* **68:** 201–219

Strigini M (2005) Mechanisms of morphogen movement. *J Neurobiol* **64:** 324–333

Strigini M, Cohen SM (2000) Wingless gradient formation in the *Drosophila* wing. *Curr Biol* **10:** 293–300

Struhl G, Struhl K, Macdonald PM (1989) The gradient morphogen bicoid is a concentration-dependent transcriptional activator. *Cell* **57:** 1259–1273

Tabata T (2001) Genetics of morphogen gradients. *Nat Rev Genet* **2:** 620–630

Tabata T, Takei Y (2004) Morphogens, their identification and regulation. *Development* **131:** 703–712

Tabin C, Wolpert L (2007) Rethinking the proximodistal axis of the vertebrate limb in the molecular era. *Genes Dev* **21:** 1433–1442

Tanaka Y, Okada Y, Hirokawa N (2005) FGF-induced vesicular release of Sonic hedgehog and retinoic acid in leftward nodal flow is critical for left–right determination. *Nature* **435:** 172–177

Tarchini B, Duboule D (2006) Control of *Hoxd* genes' collinearity during early limb development. *Dev Cell* **10:** 93–103

Teleman AA, Cohen SM (2000) Dpp gradient formation in the *Drosophila* wing imaginal disc. *Cell* **103:** 971–980

Teleman AA, Strigini M, Cohen SM (2001) Shaping morphogen gradients. *Cell* **105:** 559–562

Tickle C (1999) Morphogen gradients in vertebrate limb development. *Semin Cell Dev Biol* **10:** 345–351

Tucker JA, Mintzer KA, Mullins MC (2008) The BMP signaling gradient patterns dorsoventral tissues in a temporally progressive manner along the anteroposterior axis. *Dev Cell* **14:** 108–119

Turing AM (1952) The chemical basis of morphogenesis. *Philos Trans R Soc London* **237:** 37–72

Umulis DM, Serpe M, O'Connor MB, Othmer HG (2006) Robust, bistable patterning of the dorsal surface of the *Drosophila* embryo. *Proc Natl Acad Sci USA* **103:** 11613–11618

Vincent JP, Dubois L (2002) Morphogen transport along epithelia, an integrated trafficking problem. *Dev Cell* **3:** 615–623

White RJ, Nie Q, Lander AD, Schilling TF (2007) Complex regulation of cyp26a1 creates a robust retinoic acid gradient in the zebrafish embryo. *PLoS Biol* **5:** e304

Wolpert L (1969) Positional information and the spatial pattern of cellular differentiation. *J Theor Biol* **25:** 1–47

Zhu AJ, Scott MP (2004) Incredible journey: how do developmental signals travel through tissue? *Genes Dev* **18:** 2985–2997